YIELD MECHANISM CURVES FOR LOCAL BUCKLING OF AXIALLY COMPRESSED MEMBERS

By

M. IVÁNYI

Department of Steel Structures, Technical University, Budapest
(Received: November 15, 1978)

1. Introduction

In examining the plastic load capacity of steel structures, beside strength characteristics of members, also the analysis of deformation capacity is of importance. The deformation capacity is characterized by the load-displacement relation of the members. The deformation capacity is exhausted if increasing displacements belong to decreasing loads leading to failure of the member (Fig. 1).

Similar to load capacity, also deformation capacity depends on several factors such as changes in the geometry of the structure (column buckling, lateral buckling) or in the geometry of the cross section (local buckling). In what follows, cross sectional changes of compressed members will be considered.

The member is assumed to be in plastic range and premature buckling of the plates constituting its cross section counteract the unrestricted plastic deformations. The problem is to determine yield mechanism curves due to buckling of constituting plates.

2. Preliminary research

Plate buckling is influenced by plate geometry and by the supporting action of adjacent plate parts, these being the two basic factors for the problem of deformation capacity. Tests by HAAIJER, G. [1] were based on the discontinuous yield properties of steel. The differential equation of the equilibrium of orthotropic plates was applied to plates in the plastic range with different supports; various coefficients in the equation were determined experimentally.

LAY, M. G. [2] examined mainly the effect of flange buckling. He established a mathematical model for compressed flanges under yield stress supported by the web by means of fictitious torsional springs. The failure was assumed to occur in form of pure torsional buckling of the rectangular flange.

Both Haaijer, G. and Lay, M. G. assumed the plate buckling problem to be solved as bifurcation of equilibrium. BEN KATO [3] tackled the problem from a different aspect.

Incipient yield of real plates with rather low thickness to width ratios is accompanied by fine "crumplings" (waviness). No drop in load capacity takes place at once but yield load is maintained during a certain deformation depending on the plate geometry and on the steel strength characteristics.

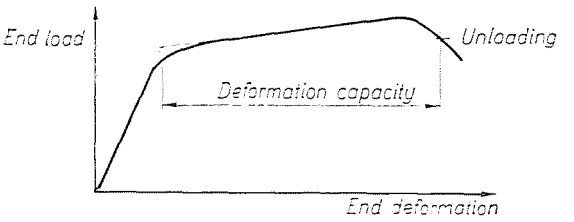

Fig. 1

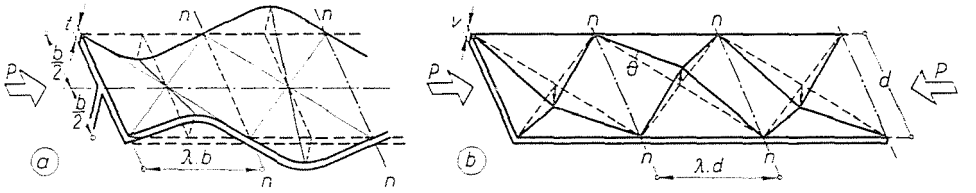

Fig. 2. a) Flange buckling; b) Web buckling

This behaviour may be attributed to the possibility of arbitrary deformations in the plate at the yield stress, since the yield plateau exhibits no unambiguous relationship between stress and strain.

"Crumpling" itself may be considered as a yield mechanism where in the plastic hinges not constant but increasing "ultimate moments" develop due to strain hardening. Load capacity — or rather deformation capacity — gets exhausted where the quoted "ultimate moment" ceases to increase. This was assumed by Ben Kato to occur at the ultimate tensile stress rather than at the yield stress in the plastic hinges. This approach permits to establish a relation between maximum compression and plate geometry. His tests involved separate analysis of flanges and web plate of the I-section, assuming separate yield mechanisms for each constituting plate, omitting the effect of elastic deformations as well. For the yield mechanism, the strain energy consisting of the bending moment and shear force energies at the plastic hinges, and the potential energy, product of compressive force by the compression, were established.

His relationships permit to put restriction on plate geometry ensuring adequate deformation capacity for the member.

Shapes assumed for the yield mechanism of the flanges and web are seen in Figs 2a and b, respectively.

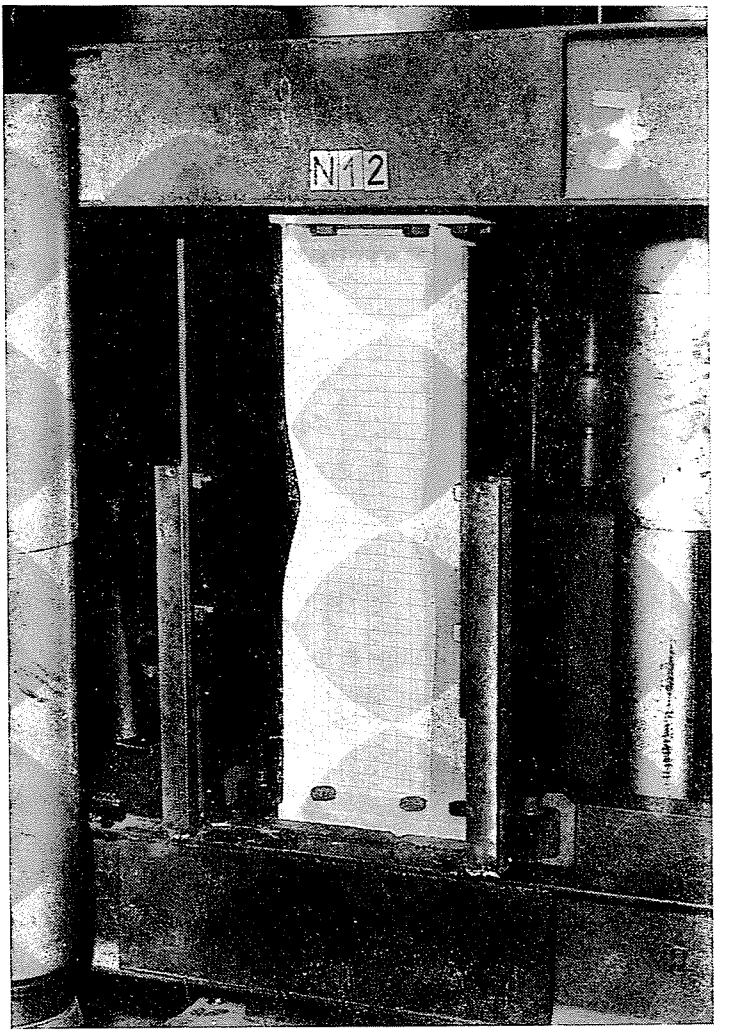

Fig. 3

A major deficiency of Ben Kato's model is the assumption of geometrically independent buckling configuration in the constituting plates of the I-section.

Even the form of the specimen seen in Fig. 3 demonstrates buckling configuration of the flanges and the web not to be independent geometrically.

3. Basic method and a simple example

Among the extreme value theorems of plasticity, the kinematic theorem [4] giving an upper limit will be applied.

Thus, a yield mechanism will be adopted such as to correspond to the geometrical conditions and the assumed yield criterion. In addition to Ben Kato, this method has been applied by ALEXANDER, I. M. [5], PUGESLEY, A.

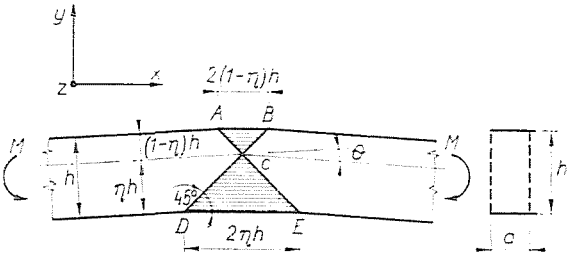

Fig. 4

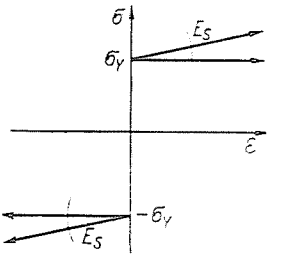

Fig. 5

and MACAULAY, M. [6] for examining cylindrical shells, while by CLIMENHAGA, J. J. and JOHNSON, P. [7] for the analysis of buckling due to the negative moment of the steel beam component of composite beams.

The method will be illustrated by a simple example (Fig. 4). Let us take a bar of an isotropic, incompressible, rigid-plastic material (Fig. 5), subject to the Tresca yield condition. Rigid and plastic zones include an angle of 45° with the bar axis. For a small rotation θ, in the plastic hinge (yield mechanism) deformations of identical magnitude but opposite sign develop in directions x and y, while incompressibility requires zero strain in direction $z(\varepsilon_z = 0)$. According to the yield criterion, stresses in directions y and z are zero $(\sigma_y = \sigma_z = 0)$ while in direction x they equal the yield point $(\sigma_x = \pm\sigma_Y)$.

Centre of rotation c is located as a function of depth h. Writing deformation energy of the plastic hinge (yield mechanism):

$$W_a = V \int_{(\varepsilon)} \sigma \cdot d\varepsilon \tag{1}$$

where

$$V = \left(\frac{2\eta^2 h^2}{2} + \frac{2(1-\eta)^2 h^2}{2}\right) a = (1 - 2\eta + 2\eta^2)\, h^2 a .$$

$V =$ minimum for $\eta = 0.5$, hence

$$V = \frac{ah^2}{2} . \tag{2}$$

For a small rotation θ, because of the 45° limit, the strain becomes

$$\varepsilon_x = \pm \frac{\theta}{2} \tag{3}$$

$$W_a = V \int_0^{\varepsilon_x} \sigma_x \, d\varepsilon = \frac{ah^2}{2} \int_0^{\theta/2} \sigma_Y d\varepsilon = \frac{ah^2}{2} \theta \frac{\sigma_Y}{2} . \tag{4}$$

The potential energy:

$$W_h = \int_{\theta} M \cdot d\theta. \tag{5}$$

Equating deformational and potential energies:

$$\int_{\theta} M \cdot d\theta = \frac{ah^2}{4} \sigma_Y \, \theta. \tag{6}$$

Deriving Eq. (6) with respect to θ:

$$M = \frac{ah^2}{4} \sigma_Y . \tag{7}$$

In case of a strain-hardening material (Fig. 5):

$$\sigma_x = \sigma_Y + \varepsilon_x \cdot E_s. \tag{8}$$

Substituting (8) into (4) and (5):

$$M = \frac{ah^2}{2} \left(\sigma_Y + \frac{1}{2} \theta \, E_s \right) . \tag{9}$$

The presented method suits also more complicated cases.

4. Yield mechanism curves

The yield mechanism adopted according to experimental data is seen in Fig. 6.

Shaded areas undergo plastic deformation; if their — undeformed — boundaries include an angle of 45° with the bar axis, then the model according to Chapter 3 may be applied, valid also for the heavy lines in the figure, considered as linear plastic hinges. Yield points of web and flanges σ_Y are assumed not to be equal but in any case the strain-hardening modulus is E_s.

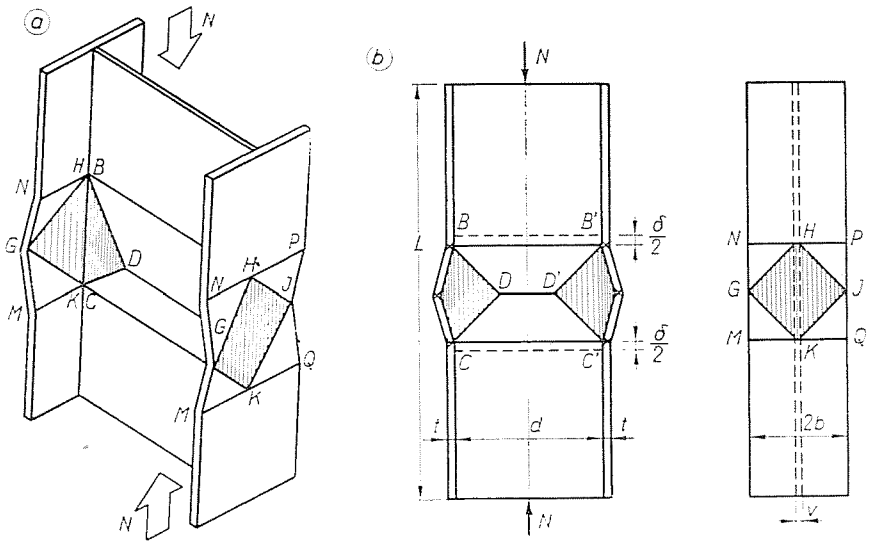

Fig. 6. σ_{Yf} = yield stress of the flange; σ_{Yw} = yield stress of the web; E = Young's modulus; E_s = secant strain-hardening modulus

Plastic strain in the web plate develops in zones BCD and B'C'D', with the development of plastic hinges BD, B'D', CD, C'D', BB', CC' and DD'.

In the web plate (its behaviour is assumed to be symmetric about the bar axis), plastic strain develops in the zone KGHJ, with the development of plastic hinges MK, KQ, NH, HP and GK, GH, JK, JH.

Yield mechanism of the web plate is compatible with those of the flanges if points B and C coincide with H and K, making the yield mechanism of the entire section determinate. Now, deformational and potential energies may be written for the yield mechanism of the plate parts (Appendix).

As a conclusion:

$$\int_{\delta} N d\delta = W_a = 2W_{BCD} + 2W_{BB'} + W_{DD'} + 4W_{BD} + \\ + 2W_{KJ} + 2W_{NH} + 2W_{GG} + 2W_{BC}. \tag{10}$$

Value of force N is found by differentiating the equation:

$$N = \frac{dW_a}{d\delta} = 2\frac{dW_{BCD}}{d\delta} + 2\frac{dW_{BB'}}{d\delta} + \frac{dW_{DD'}}{d\delta} + 4\frac{dW_{BD}}{d\delta} + \\ + 2\frac{dW_{KJ}}{d\delta} + 2\frac{dW_{NH}}{d\delta} + 2\frac{dW_{GG}}{d\delta} + 2\frac{dW_{BC}}{d\delta}. \tag{11}$$

Also data of the yield mechanism of plate parts $\frac{dW}{d\delta}$ are seen in the Appendix.

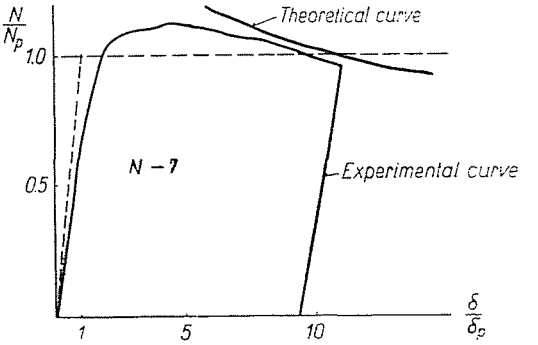

Fig. 7. Specimen *N*-7. Web: $200-5\left(\frac{d}{v}=40\right)$; Flanges: $120-5\left(\frac{b}{t}=26.6\right)$; $\sigma_{Yw}=2400\,\mathrm{kp/cm^2}$ (240 MPa); $\sigma_{Yf}=2400\,\mathrm{kp/cm^2}$ (240 MPa); $E_s=1250\,\mathrm{kp/cm^2}$ (125 MPa)

Eq. (11) may be made dimensionless by introducing:

$$N_p = 4b \cdot t \cdot \sigma_{Yf} + d \cdot v \cdot \sigma_{Yw} \tag{12}$$

$$\delta_Y = \frac{N_p \cdot L}{E(4bt + dv)} \tag{13}$$

$$\frac{N}{N_p} = \frac{1}{N_p} \cdot \frac{dW_a}{d\delta}. \tag{14}$$

Knowing geometrical data and material characteristics, assuming different δ and δ/δ_Y values, N and N/N_p defining the yield mechanism curves of a given bar can be determined as illustrated in Fig. 7.

Our analyses involved several approximations making the assumed stress and strain condition to be only valid for slight displacements although some plastic hinges may develop great rotations, which are thus to be limited [7]. Reduction of the moment in the plastic hinges due to simultaneous compressive force has been neglected.

Also the secondary effect from the spatial condition of the yield mechanism has been neglected.

Validity of approximations applied in the determination of the yield mechanism curve, rather simple to manage, has been confirmed by test results.

5. Experimental checking

In 1977, in the Laboratory of the Department of Steel Structures a theoretical and experimental project has been launched to examine plastic plate buckling [8].

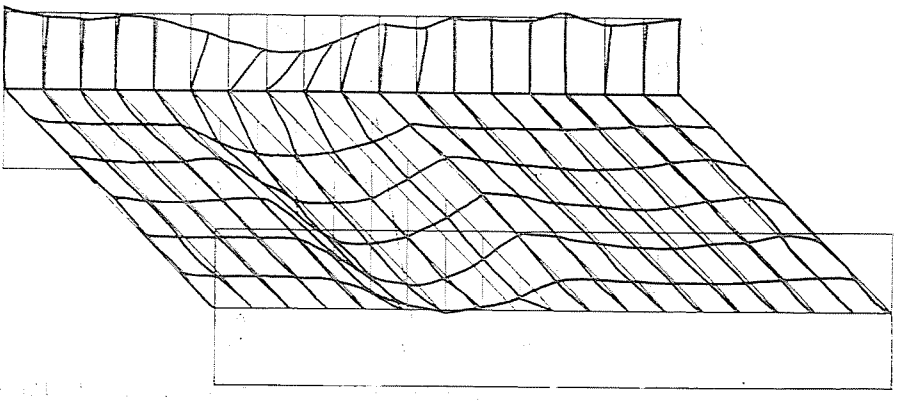

Fig. 8. Deflections of the web and of one flange of specimen *N*-7

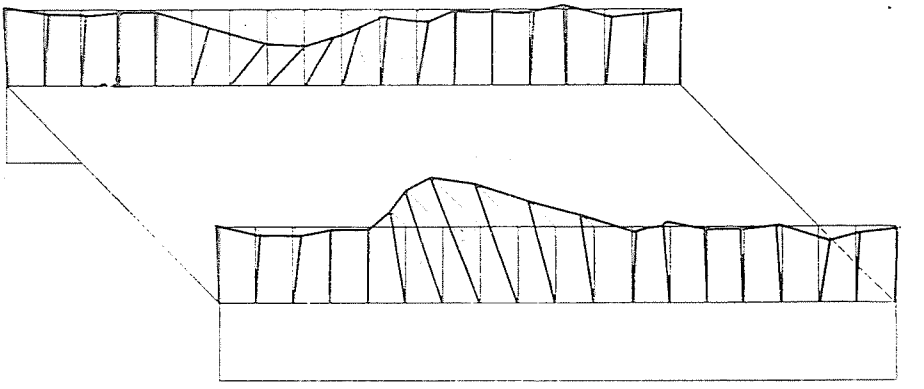

Fig. 9. Flange deflections of specimen *N*-7

Among results with the specimens, those for No. *N*-7 will be presented.

The dimensionless curve $N-\delta$ is seen in Fig. 7, together with the yield mechanism curve.

The buckled forms of web and flange are seen in Figs 8 and 9.

Test results confirm theoretical assumptions. For given plate proportions, web and flange buckling figures are not geometrically independent.

The assumed flange buckling wave length in Fig. 6 was 120 mm, against the experimental 128 mm.

Summary

By means of yield mechanism curves the effect of plastic buckling of plates in compressed members can be analysed. Yield mechanism curves permit to choose cross section to possess the adequate deformation capacity needed for a favourable structural behaviour, of great importance in the plastic design of steel structures.

References

1. HAAIJER, G.: Plate Buckling in the Strain-Hardening Range, J. ASCE Vol. 83. EM2. April, 1957.
2. LAY, M. G.: Flange Local Buckling in Wide-Flange Shapes. J. ASCE Vol. 91. ST. 6, Dec. 1965.
3. BEN KATO: Buckling Strength of Plates in the Plastic Range. Publications of IABSE, Vol. 25. 1965.
4. KALISZKY, S.: Plasticity, Theory and Engineering Applications.* Akadémiai Kiadó Budapest 1975.
5. ALEXANDER J. M.: An Approximate Analysis of the Collapse of Thin Cylindrical Shells Under Axial Loading. Quarterly Jrl. of Mechanical and Applied Mathematics Vol. 13, 1960.
6. PUGESLEY A.—MACAULAY M.: The Large-Scale Crumpling of Thin Cylindrical Columns. Quarterly Jrl. of Mechanical and Applied Mathematics Vol. 13, 1960.
7. CLIMENHAGA, J. J.—JOHNSON, P.: Moment-Rotation Curves for Locally Buckling Beams. J. ASCE Vol. 98, ST 6. June 1972.
8. IVÁNYI, M.: Limits of Plate Slenderness in Plastic Design. Final Report; Regional Colloquium on Stability of Steel Structures, Hungary, 1977.

Appendix

Strain energies of yield mechanisms of plate parts are:

A.1 Web plate (Figs A. 1 and A. 2)

A.1.1 Plastic zones BCD and B'C'D'

BCD and B'C'D' are strains in direction of the compressive force:

$$\varepsilon = \frac{\delta}{2b}. \tag{A.1}$$

Utilizing characteristics of the rigid—strain-hardening material, the strain energy becomes:

$$W_{BCD} = V_{BCD} \int_0^{\delta/2b} (\sigma_{Yw} + \varepsilon \cdot E_s)\, d\varepsilon =$$

$$= vb^2 \left\{ \sigma_{Yw} \left(\frac{\delta}{2b} \right) + \frac{1}{2} \left(\frac{\delta}{2b} \right)^2 E_s \right\} = vb \left\{ \sigma_{Yw} + \frac{\delta E_s}{4b} \right\} \frac{\delta}{2}. \tag{A.2}$$

Differentiating:

$$\frac{dW_{BCD}}{d\delta} = vb \left\{ \sigma_{Yw} + \frac{\delta \cdot E_s}{2b} \right\} \frac{1}{2} = \frac{dW_{B'C'D'}}{d\delta}. \tag{A.3}$$

A.1.2 Plastic hinges BB' and CC'

First, the hinge rotation angle due to the assumed yield mechanism has to be determined. Section X-X indicated in Fig. A.1 is seen in Fig. A.3 showing hinges CC' and BB' to rotate by α:

$$g = 2b - \delta \tag{A.4}$$

$$\cos \alpha = \frac{g}{2b} = 1 - \frac{\delta}{2b} \tag{A.5}$$

$$\sin \alpha = \sqrt{1 - \left(1 - \frac{\delta}{2b}\right)^2} \tag{A.6}$$

$$\alpha = \arccos \left(1 - \frac{\delta}{2b}\right). \tag{A.7}$$

* In Hungarian.

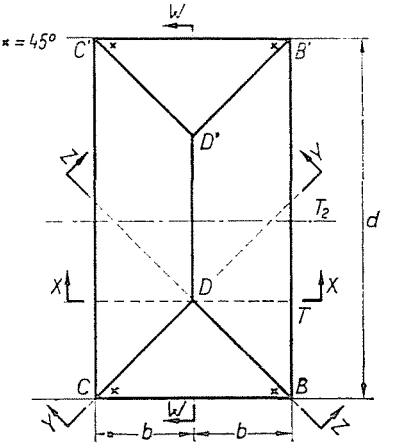

Fig. A1

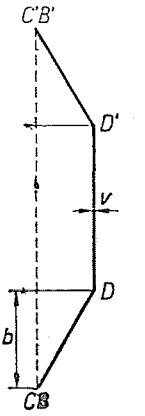

Fig. A2. Section $W-W$

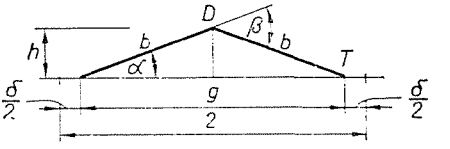

Fig. A3. Section $X-X$

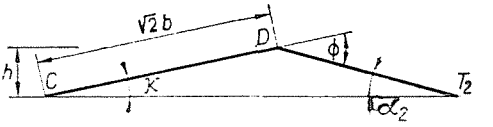

Fig. A4. Section $Y-Y$

To obtain the derivatives of α with respect to δ:

$$\frac{d\alpha}{d\delta} = \frac{1}{2b} \cdot \frac{1}{\sin \alpha} . \tag{A.8}$$

For a small rotation ε. the axial strain was as demonstrated in Chapter 3:

$$\varepsilon = \frac{\alpha}{2} . \tag{A.9}$$

The strain energy:

$$W_{BB'} = V_{BB'} \int_0^{\alpha/2} (\sigma_{Yw} + \varepsilon E_s)\, d\varepsilon = \frac{1}{2} v^2 d \left\{ \sigma_{Yw} + \frac{\alpha E_s}{4} \right\} \frac{\alpha}{2} . \tag{A.10}$$

The derivative with respect to δ utilizing (A.8):

$$\frac{dW_{BB'}}{d\delta} = \frac{1}{4} v^2 d \left\{ \sigma_{Yw} + \frac{\alpha E_s}{2} \right\} \left\{ \frac{d\alpha}{d\delta} \right\} = \frac{dW_{CC'}}{d\delta} . \tag{A.11}$$

A.1.3 *Plastic hinge DD'*

The plastic hinge rotates by β, according to Fig. *A3*: $\beta = 2\alpha$ the strain being:

$$\varepsilon = \frac{\beta}{2} = \alpha \tag{A.12}$$

and the strain energy:

$$W_{DD'} = V_{DD'} \int_0^{\alpha} (\sigma_{Yw} + \varepsilon \cdot E_s) d\varepsilon = \frac{1}{2} v^2 (d - 2b) \left\{ \sigma_{Yw} + \frac{\alpha \cdot E_s}{2} \right\} \alpha. \tag{A.13}$$

Its derivative with respect to δ, utilizing (A8):

$$\frac{dW_{DD'}}{d\delta} = \frac{1}{2} v^2 (d - 2b) \{ \sigma_{Yw} + \alpha \cdot E_s \} \left\{ \frac{d\alpha}{d\delta} \right\}. \tag{A.14}$$

A.1.4 *Plastic hinges BD; CD and B'D'; C'D'*

Sections *Y-Y* and *Z-Z* in Fig. *A1* are seen in Fig. *A4* where the plastic hinge rotates by:

$$\Phi = \varkappa + \alpha_2.$$

Due to geometry: $\varkappa = \alpha_2$

$$\sin \varkappa = \frac{h}{\sqrt{2}b} = \frac{\sin \alpha}{\sqrt{2}} \tag{A.15}$$

since $h = b \cdot \sin \alpha$ (from section *X-X*):

$$\varkappa = \arcsin \left\{ \frac{\sin \alpha}{\sqrt{2}} \right\} \tag{A.16}$$

$$\Phi = 2 \arcsin \left\{ \frac{\sin \alpha}{\sqrt{2}} \right\}. \tag{A.17}$$

In need of the derivative of $\sin \alpha$ with respect to δ:

$$\frac{d(\sin \alpha)}{d\delta} = \frac{\cos \alpha}{\sin \alpha} \cdot \frac{1}{2b} \tag{A.18}$$

and the derivative of Φ with respect to δ:

$$\frac{d\Phi}{d\delta} = \frac{1}{\sqrt{2}} \cdot \frac{1}{\cos \varkappa} \cdot \frac{d(\sin \alpha)}{d\delta}. \tag{A.19}$$

Plastic hinge strain:

$$\varepsilon = \frac{\Phi}{2}. \tag{A.20}$$

The strain energy:

$$W_{BD} = V_{BD} \int_0^{\Phi/2} (\sigma_{Yw} + \varepsilon E_s)\, d\varepsilon = \frac{\sqrt{2}\, bv^2}{2} \left\{ \sigma_{Yw} + \frac{\Phi E_s}{4} \right\} \frac{\Phi}{2}. \tag{A.21}$$

The derivative with respect to δ, utilizing (A.18) and (A.19):

$$\frac{dW_{BD}}{d\delta} = \frac{\sqrt{2}}{4} bv^2 \left\{ \sigma_{Yw} + \frac{\Phi E_s}{2} \right\} \left\{ \frac{d\Phi}{d\delta} \right\} = \frac{dW_{CD}}{d\delta} = \frac{dW_{B'D'}}{d\delta} = \frac{dW_{C'D'}}{d\delta}. \tag{A.22}$$

A.2 Flange plate (Fig. *A5*)

A.2.1 Plastic zone KGHJ:

The strain:

$$\varepsilon = \frac{\delta}{2b} .$$

The strain energy:

$$W_{KJ} = V_{KJ} \int_0^{\delta/2b} (\sigma_{Yf} + \varepsilon E_s) d\varepsilon = 2b^2 t \left\{ \sigma_{Yf} \left(\frac{\delta}{2b} \right) + \frac{1}{2} \left(\frac{\delta}{2b} \right)^2 E_s \right\} =$$

$$= bt \left\{ \sigma_{Yf} + \frac{\delta \cdot E_s}{2b} \right\} \delta . \tag{A.24}$$

Differentiating:

$$\frac{dW_{KJ}}{d\delta} = bt \left\{ \sigma_{Yf} + \frac{\delta E_s}{2b} \right\} . \tag{A.25}$$

A.2.2 Plastic hinges NH, HP, QK and KM

Section U—U in Fig. *A5* is seen in Fig. *A6* where plastic hinges NH, HP, QK and KM rotate by:

$$h_1 = \sqrt{b\delta - \frac{\delta^2}{4}} \tag{A.26}$$

$$\sin \varrho = \frac{h_1}{b} = \frac{\sqrt{b\delta - \frac{\delta^2}{4}}}{b} \tag{A.27}$$

$$\varrho = \arcsin \left\{ \frac{\sqrt{b\delta - \frac{\delta^2}{4}}}{b} \right\} . \tag{A.28}$$

The derivative of ϱ with respect to δ.

$$\frac{d\varrho}{d\delta} = \frac{1}{\cos \varrho} \cdot \frac{1}{2b} \cdot \frac{b - \frac{\delta}{2}}{\sqrt{b\delta - \frac{\delta^2}{4}}} \tag{A.29}$$

Strain in the plastic hinge:

$$\varepsilon = \frac{\varrho}{2} . \tag{A.30}$$

Strain energy:

$$W_{NH} = V_{NH} \int_0^{\varrho/2} (\sigma_{Yf} + \varepsilon E_s) \, d\varepsilon = 2bt^2 \left\{ \sigma_{Yf} + \frac{\varrho E_s}{4} \right\} \frac{\varrho}{2} . \tag{A.31}$$

The derivative with respect to δ utilizing (A.29):

$$\frac{dW_{NH}}{d\delta} = bt^2 \left\{ \sigma_{Yf} + \frac{\varrho E_s}{2} \right\} \left\{ \frac{d\varrho}{d\delta} \right\} = \frac{dW_{HP}}{d\delta} = \frac{dW_{QK}}{d\delta} = \frac{dW_{KM}}{d\delta} . \tag{A.32}$$

A.2.3 Plastic hinges GH, HJ, JK and KG

Section $V-V$ in Fig. *A5* is seen in Fig. *A7*, with the plastic hinge rotating by:

$$2\lambda\,.$$

Due to geometry:

$$h_2 = \frac{h_1}{2} \tag{A.33}$$

$$\sin\lambda = \frac{\sqrt{2}\,h_2}{b} = \frac{\sqrt{2}}{2}\sin\varrho \tag{A.34}$$

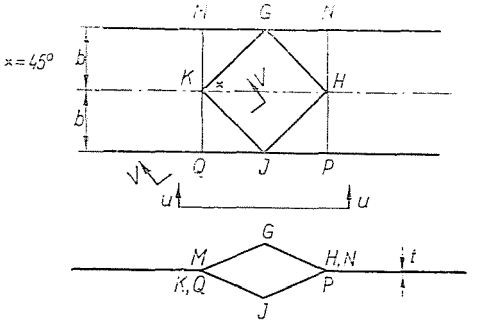

Fig. A5

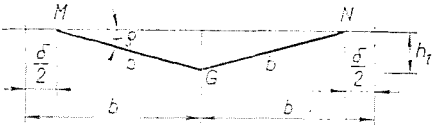

Fig. A6. Section $M-N$

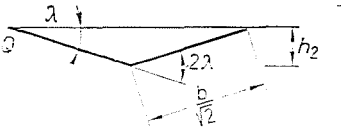

Fig. A7. Section $V-V$

$$\lambda = \text{arc}\sin\left\{\frac{\sqrt{2}}{2}\sin\varrho\right\}. \tag{A.35}$$

The derivative of λ with respect to ϱ, utilizing (A.29):

$$\frac{d\lambda}{d\delta} = \frac{1}{\cos\lambda}\cdot\frac{\sqrt{2}}{2}\cdot\cos\varrho\left\{\frac{d\varrho}{d\delta}\right\}. \tag{A.36}$$

Plastic hinge strain:

$$\varepsilon = \frac{2\lambda}{2} = \lambda. \tag{A.37}$$

Strain energy for the four hinges:

$$W_{GG} = V_{GG}\int_0^{\lambda}(\sigma_{Yf} + \varepsilon\cdot E_s)d\varepsilon = 2\sqrt{2}\,bt^2\left\{\sigma_{Yf} + \frac{\lambda E_s}{2}\right\}\lambda. \tag{A.38}$$

Derivative with respect to δ, utilizing (A.36):

$$\frac{dW_{GG}}{d\delta} = 2\sqrt{2}\,bt^2\left\{\sigma_{Yf} + \frac{\lambda E_s}{2}\right\}\left\{\frac{d\lambda}{d\delta}\right\}. \tag{A.39}$$

A.3 Plastic hinges BC and B'C'

Plastic hinge developing between the web and the flange — or assumed in the web plate — is seen in Fig. *A8*.
Plastic hinge rotation:

$$\omega = \varrho - \arcsin\left\{\frac{b \cdot \sin\alpha}{b}\right\} \tag{A.40}$$

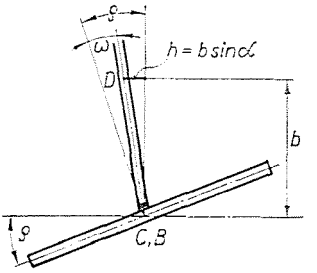

Fig. A8. Section $W-W$

$$\omega = \varrho - \alpha. \tag{A.41}$$

Derivative with respect to δ:

$$\frac{d\omega}{d\delta} = \frac{d\varrho}{d\delta} - \frac{d\alpha}{d\delta}. \tag{A.42}$$

Plastic hinge strain:

$$\varepsilon = \frac{\omega}{2}. \tag{A.43}$$

Strain energy:

$$W_{BC} = V_{BC}\int_0^{\omega/2}(\sigma_{Yw} + \varepsilon E_s)\,d\varepsilon = v^2 b\left\{\sigma_{Yw} + \frac{\omega E_s}{4}\right\}\cdot\frac{\omega}{2} \tag{A.44}$$

$$\frac{dW_{BC}}{d\delta} = \frac{v^2 b}{2}\left\{\sigma_{Yw} + \frac{\omega E_s}{2}\right\}\left\{\frac{d\omega}{d\delta}\right\} = \frac{dW_{B'C'}}{d\delta}. \tag{A.45}$$

Associate Prof. Dr. Miklós IVÁNYI, H-1521 Budapest